

CHAPTER 210

WAVE-CURRENT INTERACTION WITH MUD BED

Nguyen Ngoc An¹
Tomoya Shibayama²

ABSTRACT

A series of wave flume experiments for wave-current-mud system has been performed. The results reveal that the rate of wave attenuation increases in the opposing currents and decreases in the following currents. The results are the same with the waves on the fixed bed. Another important result is that the mud mass transport velocity increases in the opposing currents and decreases in the following currents. The visco-elastic-plastic model which was proposed by Shibayama and An (1993) for wave-mud interaction has further been extended to the wave-current-mud system by taking a wave deformation effect into considerations. The extended model succeeds in predicting the laboratory results. The model shows that due to pressure gradient in wave propagating direction, the largest mud mass transport velocity occurs in the strongest opposing current and the smallest one in the strongest following current.

INTRODUCTION

The wave-current interaction is a phenomenon of considerably practical interest. Also waves traveling on mud bed is another important phenomenon because these results in high wave attenuation (Gade, 1958 and Tubman and Suhayda, 1976) and large mud mass transport (Sterling and Strohbeck, 1973).

¹ D. Eng., Department of Civil Engineering, HCMC University of Technology

² D. Eng., Associate Professor, Department of Civil Engineering, Yokohama National University

The wave-current interactions on fixed bed have been studied through both laboratory experiments and mathematical analyses (Brevik and Aas, 1980, Thomas, 1981, etc.). And it is known that currents introduced into wave field make change of wavelength and wave height. The wave-current interactions on the mud bed have not yet been studied well, and therefore their effects on the mud mass transport velocity and the wave attenuation remain unclarified. In order to evaluate wave attenuation rate under this condition, Nakano et al. (1989) tried to include current effect to their multi-layered viscous fluid model (Tsuruya et al., 1987). But the results are not well compared with their own laboratory data.

These interactions among wave, current and mud will be investigated through both laboratory experiments and the numerical model in the present study.

THEORETICAL CONSIDERATIONS

It is understood that the pressure gradient of water waves is much more important than shear stress at the interface between the water layer and the mud layer in creating movement of mud in the mud bed. In the mathematical formulation, it is assumed that the wave attenuation process will take place after waves are deformed due to the currents. This means that the mud bed responds only to the deformed waves resulting by the wave-current interaction. This assumption will be later justified with the laboratory experiments. It is also assumed that the current itself has no effect on the mud mass transport in the bed layer. The experimental results of Otsubo and Muraoka (1986a) can be used to justify the latter assumption. It was found that when currents flow over mud bed, sediments are transported only in the water layer by the current if they are suspended or if the bed surface is massively destroyed. No mass transport in the mud layer was reported. In the followings, two models which describe the two processes will be present.

Model of Wave Deformation due to Current

In this process, no energy loss is taken into account while formulating the model of wave deformation due to the currents. Two main parameters of deformed waves are the wave height and the wavelength. The accuracy in

predicting the wavelength variation using the dispersion relation has been verified (Thomas, 1981). The accuracy in predicting the wave height variation, however, depends on the nature of currents. Several models are available. Longuet-Higgins and Stewart (1961,1964) assumed that the current was irrotational and its profile was uniform over depth. Jonsson et al. (1978) solved for rotational currents by assuming current with constant vorticity. Thomas (1981) numerically solved for more general case by considering current to be a function of elevation from bottom. In a simple case where the depth-averaged velocity was used, he found that the model well predicted the wavelength and wave height variations.

Under steady condition following Thomas (1981) for the simple case, the conservation equation for wave action is (Bretherton and Garrett, 1969; Whitham, 1974; Brevik and Aas, 1980)

$$\frac{E}{\sigma}(U + C_{gr}) = \text{const.} \quad (1)$$

where E is the wave energy, σ is the relative angular frequency defined by $\sigma = \omega - kU$, ω is the absolute angular frequency, U is the mean depth-averaged current velocity, k is the wave number, and C_{gr} is the group wave velocity. Because the wave energy is proportional to the square of wave height, H , Eq. (1) can be rewritten as:

$$\frac{H^2}{\sigma}(U + C_{gr}) = \text{const.} \quad (2)$$

The wavelength variation is obtained from the usual irrotational dispersion relation as follows:

$$(\omega - kU)^2 - gk \tanh kd_i = 0 \quad (3)$$

where d_i is the water depth. Following Thomas (1981), in order to use Eqs. (2) and (3), it is necessary to specify a reference level to define the constant in Eq. (2). The reasonable choice of reference level is the values with no current. This introduces the quantities H_0 and L_0 , corresponding to the wave height and the wavelength respectively when no current exists.

Model of Wave-Current Interaction on the Mud Bed

The model of wave-mud interaction which was developed by Shibayama and An (1993) is used. In this process, the model of wave-mud system is extended

to the wave-current-mud system by taking the wave deformation effect into consideration. For example, the free surface displacement is given by $\eta_1(x,t) = a_1 \cdot \exp[i(kx - \sigma t)]$, where a_1 is the deformed wave amplitude due to the current and determined by Eq. (2).

The rheological equation and the governing equations are modified here while making use of new parameters.

(1) Rheological equations are the followings:

$$\sigma'_{ij} = 2\mu_e e'_{ij} \tag{4}$$

$$\text{where } \mu_e = \begin{cases} \mu_1 + \frac{iG}{\omega} & \left(\frac{1}{2} \sigma'_{ij} \sigma'_{ij} \leq \tau_y^2 \right) \\ \mu_2 + \frac{\tau_y}{\sqrt{4|\Pi_e|}} & \left(\frac{1}{2} \sigma'_{ij} \sigma'_{ij} > \tau_y^2 \right) \end{cases} \tag{5}$$

and σ'_{ij} and e'_{ij} are stress and strain tensors, the prime indicates the deviator of these two tensors, the dot indicates derivative with time.

(2) Governing equations are the followings:

$$\frac{\partial \hat{u}_j}{\partial x} + \frac{\partial \hat{w}_j}{\partial z} = 0 \tag{6}$$

$$\frac{\partial \hat{u}_j}{\partial t} = -\frac{1}{\rho_j} \frac{\partial \hat{p}_j}{\partial x} + \nu_{e,j} \left(\frac{\partial^2 \hat{u}_j}{\partial x^2} + \frac{\partial^2 \hat{u}_j}{\partial z^2} \right) \tag{7}$$

$$\frac{\partial \hat{w}_j}{\partial t} = -\frac{1}{\rho_j} \frac{\partial \hat{p}_j}{\partial z} + \nu_{e,j} \left(\frac{\partial^2 \hat{w}_j}{\partial x^2} + \frac{\partial^2 \hat{w}_j}{\partial z^2} \right) \tag{8}$$

where \hat{u} and \hat{w} are the horizontal and vertical components of orbital velocities, $\nu_{e,j}$ is the kinematic viscosity of mud and \hat{p} is the dynamic pressure.

(3) The solutions are put to be the following forms:

$$\hat{u}_j(x,z,t) = u_j(z) \exp[i(kx - \sigma t)] \tag{9}$$

$$\hat{w}_j(x,z,t) = w_j(z) \exp[i(kx - \sigma t)] \tag{10}$$

$$\hat{p}_j(x,z,t) = p_j(z) \exp[i(kx - \sigma t)] \tag{11}$$

EXPERIMENTAL SET-UP AND METHODOLOGY

Set-up

The experiments were carried out in a flume at the Department of Civil Engineering of Yokohama National University, Japan. The length of the flume was 17m, the width was 0.6m and the total depth was 0.55m. The still water depth was 30cm during experiment on the fixed bed and 26.3 cm on the mud layer of 8cm. Figure 1 shows the experimental set-up with the mud bed.

Instrumentation

Wave heights were measured by means of electric capacitance wave gauges. Two sensors with distance of 50cm were installed at the movable carriage to measure water elevations at every half meter along the flume. The signals from the sensors were amplified and digitally recorded for 1030 records at the frequency of 20Hz. Using the technique introduced by Goda and Suzuki (1976), the incident and reflected waves were estimated.

Horizontal component fluid velocities were measured with a Fiber-Laser Velocimeter. Steady current velocity at one point was taken as an average value of all data recorded in certain duration.

Table 1: Wave damping coefficients in wave-current condition.

Run No.	T (s)	H (cm)	U (cm/s)	d_t (cm)	k_i (1/m)	Remarks
W1	1.01	3.49	0.00	30.0	0.0036	fixed bed
WC2	1.01	2.98	-16.00	30.0	0.0085	fixed bed
WC1	1.01	2.98	-7.34	30.0	0.0044	fixed bed
W2	1.01	2.98	0.00	30.0	0.0036	fixed bed
WC3	1.01	2.98	5.58	30.0	0.0039	fixed bed
WC4	1.01	2.98	16.65	30.0	0.0027	fixed bed
WC5	1.01	4.48	-19.11	26.3	0.1032	mud bed
WC6	1.01	4.48	-9.00	26.3	0.0840	mud bed
WW7	1.01	4.48	0.00	26.3	0.0718	mud bed
WC8	1.01	4.48	8.10	26.3	0.0624	mud bed
WC9	1.01	4.48	18.64	26.3	0.0543	mud bed

Mud mass transport velocities were measured from movement of colored mud used as a tracer. The technique introduced by Sakakiyama and Bijker (1989) was adopted.

Experimental conditions

Table 1 shows the experimental conditions of waves and currents. The mixture of 158% water content of commercial kaolinite and fresh water was used for the bed material when the experiments on the mud bed were conducted.

RESULTS

Wave height variation due to current

(1) Measurement of wave heights on fixed and mud beds.

Firstly, the reference values of wave amplitude were measured. A problem arose when the location for references was selected to ensure the condition of Eq. (2). On the fixed bed, there is no problem since the wave attenuation is expected to be small. On the mud bed, however the wave attenuation rate is rather high. In this experiment, the location for references $x=0$, was chosen at front edge of the mud layer. This selection was based on the assumption that the high wave attenuation is supposed to start when the waves come to the mud bed.

Currents were generated and the velocity profiles were measured. These currents were superimposed with progressive waves produced by the wave generator. The input data of wave period T , wave height H , and water depth d_1 were the same for all runs. The actual wave amplitudes were then measured at $x=0$ for various current velocities. The measured values of H and the corresponding predicted value of L are listed in Table 2, where the subscript 0 here indicates the condition without current generation.

(2) Results.

The experimental results on the wave height variation are shown in Table 2. Figures 2 and 3 show the wave height variation for various current speeds on the fixed bed and on the mud bed, respectively. It was seen that the strongest opposing currents yielded the biggest wave heights on both the fixed and mud beds.

Table 2: Wave height variation due to currents.

Run No.	U (cm/s)	H (cm) Measured	H (cm) Predicted	H/H_0 Measured	H/H_0 Predicted	L_0 (cm)
WC2	-16.0	3.72	3.88	1.25	1.30	113
WC1	-7.34	3.23	3.32	1.08	1.11	128
W2	0.00	2.98	2.98	1.00	1.00	139
WC3	5.58	2.78	2.79	0.93	0.93	147
WC4	16.65	2.66	2.48	0.89	0.83	162
WC5	-19.1	6.00	6.21	1.34	1.39	104
WC6	-9.00	4.91	5.11	1.10	1.14	121
WW7	0.00	4.48	4.48	1.00	1.00	134
WC8	8.10	4.07	4.07	0.91	0.91	145
WC9	18.64	3.64	3.66	0.81	0.82	159

The comparisons of the measured and predicted wave heights are showed in Table 2 and in Figs. 2 and 3. Good agreements are seen. The assumption in which the mud bed responds only to deformed wave are therefore justified.

Wave attenuation due to interaction with current

To estimate the wave attenuation quantitatively, a first approximation is to assume an exponential decay law of wave height:

$$H = H_{x=0} \exp(-kx) \quad (12)$$

where $H_{x=0}$ is the initial wave height at $x=0$, H is the wave height at x and k , is the wave attenuation rate (or wave damping coefficient). This approximation is similarly supported by theoretical and experimental investigations of Keulegan (1950) and Iwasaki and Sato (1972). Although, this is only a first approximation, it turned out to be well fitted in representing present laboratory data both on the fixed and mud beds.

(1) Wave attenuation on the fixed bed by current interaction.

Although the present work mainly deals with the mud bed, one test with fixed bed was first conducted. The purposes of this test were given as follows. The first purpose was to check the wave attenuation rate with the ones obtained in previous works. The second one was to estimate a magnitude of wave attenuation rate from which the effects of currents and the effects of mud bed can be easily distinguished in the later experiments over the mud bed.

The experimental results on the wave attenuation rate, k_i , for the case $T=1.01$ s and $H_0/L_0=0.021$, are shown in Fig. 4 and in Table 1 for several values of current speed. The values of k_i were determined on the basis of regression analysis. The vertical line lengths represent standard deviations. The small standard deviations mean that the reliability is high in evaluating the wave attenuations.

There is a clear tendency in which k_i is the greatest in the strongest opposing currents and decreases slowly with the following currents. As long as the bottom boundary layer is laminar, the increase of wave number will result in the increase of energy dissipation rate. The opposing currents made the wavelength shorter. The wave number therefore increased and the higher wave attenuation rates were seen. On the other hand, the following currents made the wavelength longer. The wave number, therefore, decreased and the lower wave attenuation rates were seen.

It should be noted that the values of k_i , around 0.004 m^{-1} , obtained in the present experiment are close to the theoretical value about 0.002 m^{-1} given by Hunt (1952). These values are, however, relatively small compared to the ones of 0.02 m^{-1} obtained by Iwasaki and Sato (1972) and of 0.01 m^{-1} by Brevik (1980). The reason for this difference can be explained as follows. The incident wave heights were used in the present work to analyse wave attenuation. The closeness of present values to the theoretical ones is reasonable as long as only progressive waves are concerned.

The results of runs W1 and W2 given in Table 1 show that the same wave attenuation rates were obtained with different wave heights. Examination of the wave conditions in these tests indicated that the bottom boundary layers were laminar because the maximum Reynolds number of 3215 in the tests was smaller than the critical one of 1.26×10^4 (Jonsson, 1966). The wave attenuation rates should, therefore, be same because they do not depend on the initial wave heights as long as the bottom boundary layers are laminar (Ippen, 1966).

(2) Wave attenuation on the mud bed due to interaction with current.

The effect of currents on the wave attenuation is again considered in this part.

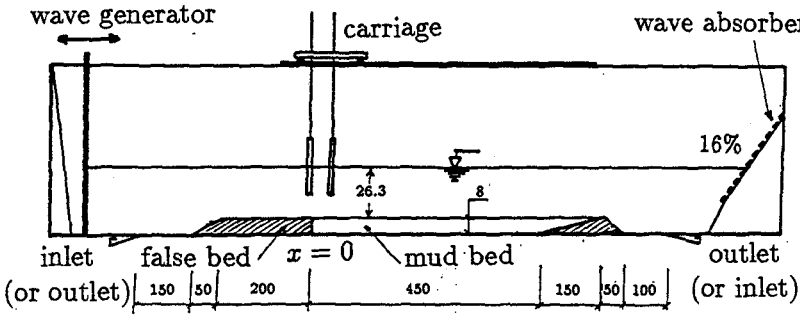


Figure 1: Sketch of experimental set-up.

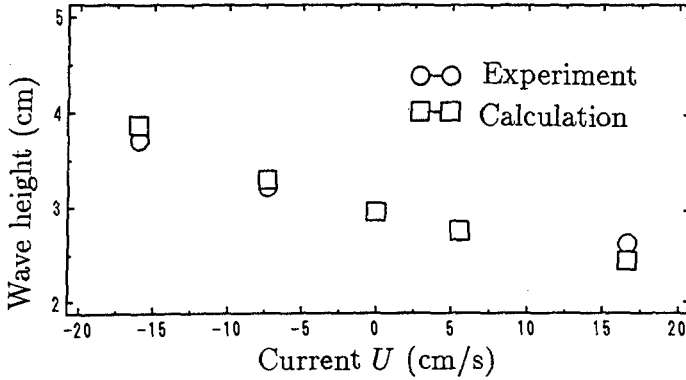


Figure 2: Wave height variation due to currents on the fixed bed.

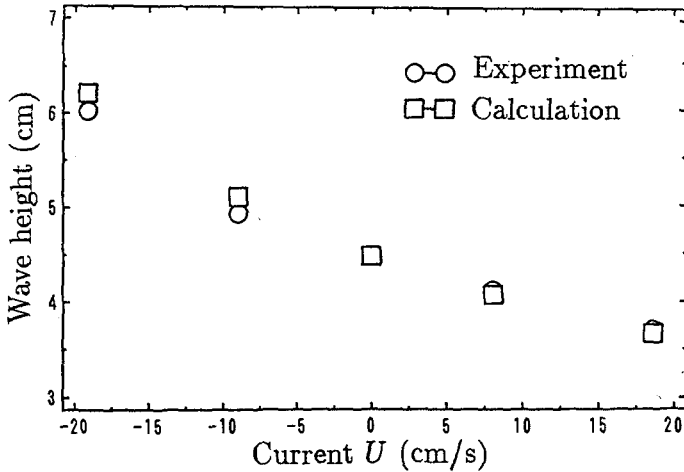


Figure 3: Wave height variation due to currents on the mud bed.

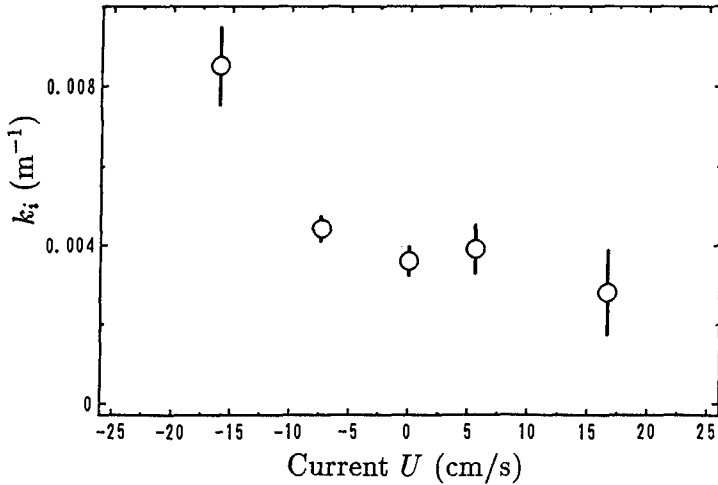


Figure 4: Effect of currents on wave attenuation on the fixed bed.

The experiments were carried out on the mud bed. Similarly, the experimental results of k_i , for the case $T=1.01s$ and $H_0/L_0=0.013$, are shown in Fig. 5 and Table 1 for several values of current velocity. The wave attenuation rate is the highest in the strongest opposing currents and decreases in the following currents, in the same manner with the waves on the fixed bed. Although the same tendency of wave attenuation are found for waves on the fixed bed and the mud bed, the magnitudes of wave attenuation for waves on the mud bed are one order of magnitude greater than the ones for waves on the fixed bed. It was confirmed again that the mud bed enhances wave attenuation.

These laboratory results are now utilized to verify the numerical model. The comparison between the laboratory data and the computed ones are shown in Fig. 5. The model predicts the highest wave attenuation rate in the strongest opposing currents and the lowest wave attenuation rate in the fastest following currents, in the same manner with the wave attenuation which varied with the current speeds observed in the experiments. In terms of the absolute magnitudes, the model also predicts well the wave attenuations in all cases of various current speeds except in the case of strongest opposing current where the model gives underestimation. The strongly nonlinear wave pattern in the strongest opposing current might be the reason for this underestimation because the model is based on the linear waves.

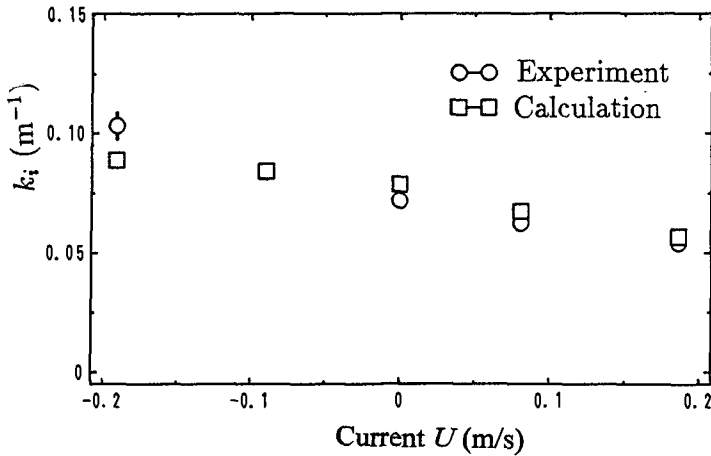


Figure 5: Effect of currents on wave attenuation on the mud bed.

Mud mass transport velocity under wave-current interaction

(1) Measurements.

The mud mass transport velocity is the average velocity obtained from the measured displacement over the duration of experiment. The duration time, therefore, was a decisive factor in determining the mud mass transport velocity. A long duration would render the mud surface slope tilted at the onshore end and less mud mass transport might be resulted. On the other hand, if a very short duration was applied, the effect of inertial force and thixotropy effect would become profound. By trial and by carefully observing the formation of mud surface slope, the proper duration was selected to be from 65 s to 75 s. For each run, the mud mass transport was measured at the location of 1.0 m downstream of the front edge of the mud layer.

(2) Mud mass transport velocity.

A series of five runs with various current speeds was performed in order to analyse the effect of currents on the mud mass transport velocity.

Before comparisons are made between the calculated results with the laboratory data some parameters used in calculation are explained here. The parameters μ_1 and G were given by Shibayama and An (1993). The values of $\mu_2 = 4.5 \text{ N s/m}^2$ and $\tau_y = 17.0 \text{ N/m}^2$ are chosen by being fitted to mud mass transport velocity and wave attenuation rate in the case of no current, and then

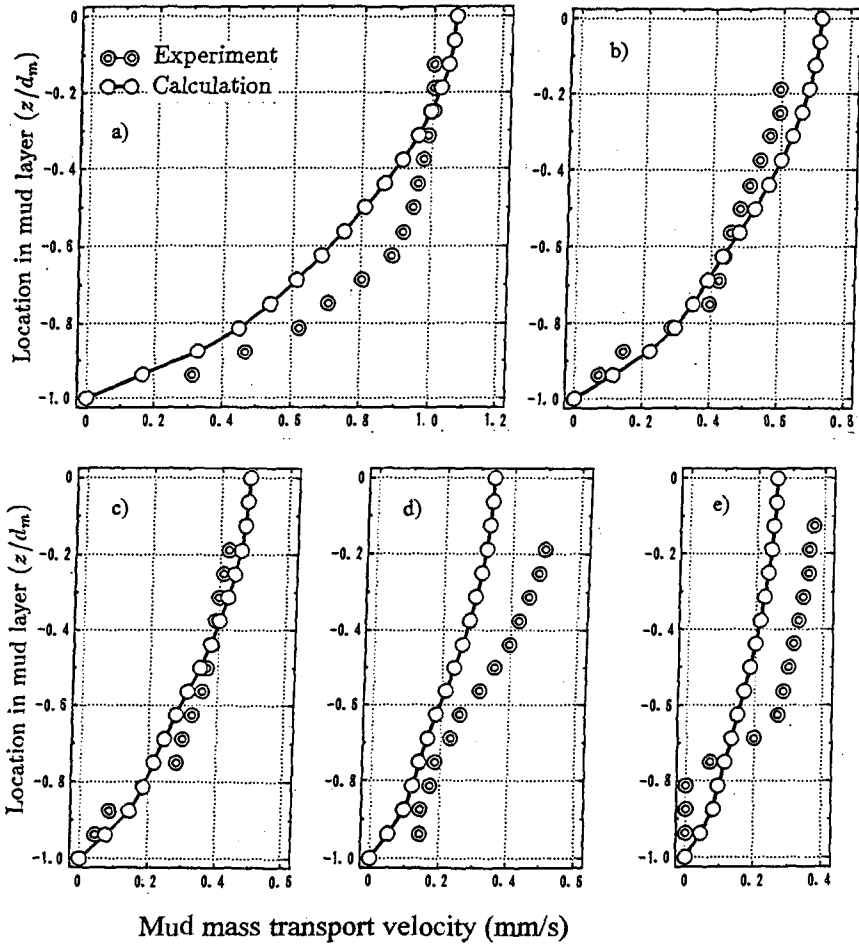


Figure 6: The comparison between the experimental and calculated results on mud mass transport velocity. a) Run WC5: $T=1.01s$, $U=-19.1 \text{ cm.s}^{-1}$, b) Run WC6: $T=1.01s$, $U=-9.0 \text{ cm.s}^{-1}$, c) Run WW7: $T=1.01s$, $U=0$, d) Run WC8: $T=1.01s$, $U=+8.1 \text{ cm.s}^{-1}$, e) Run WC9: $T=1.01s$, $U=+18.6 \text{ cm.s}^{-1}$.

applied them for other calculations with currents.

The results of mud mass transport velocity at $x=1.0\text{m}$ in five runs are shown in the Fig. 6. There is a trend that the mud mass transport velocity is biggest in the strongest opposing current and decreases with increasing current in the positive direction. This trend can also be predicted by the numerical model. The good agreement between the experimental results and the computed ones confirms that the numerical model on the wave-mud interaction can further be extended to predict the wave-current-mud interaction by taking wave deformation effect into consideration. The effect of currents on mud transport can be explained by the wave deformation due to current as follows. In the opposing currents, the water pressure gradient at the water-mud interface becomes great as the wave height increases and the wavelength decreases, and this change causes to yield large mud transport. In the following currents, the pressure gradient becomes small as the wave height decreases and the wavelength increases and this results small mud transport.

CONCLUSIONS

From the present study, some conclusions on the wave-current-mud interaction are drawn as follows.

- (1) Usage of the incident wave height improves the reliability of analysis of wave attenuations significantly.
- (2) Wave attenuation increases in the opposing currents and decreases in the following currents on both the fixed and mud bed.
- (3) Wave height variation due to wave-current interactions on the mud bed can be predicted well by a simple model of irrotational slowly-varying current.
- (4) The mud mass transport velocity increases in the opposing currents and decreases in the following currents.
- (5) The numerical model for the wave-mud interaction has further been extended for the wave-current-mud interactions by taking a wave deformation effect into consideration. The extended model succeeded in predicting the

laboratory results that the largest mud mass transport velocity and highest rate of wave attenuation occur in the strongest opposing current and the smallest and lowest ones in the fastest following current.

ACKNOWLEDGMENTS

The research reported in this paper is supported in part by the Grant-in-Aid for Scientific Research from the Japanese Ministry of Education, Science and Culture (No. 03650417) and by the research support of Penta-Ocean Construction Co. Ltd.

REFERENCES

- Bretherton, F.P. and Garrett, C.J.R. (1969): Wavetrains in inhomogeneous moving media, *Proc. R. Soc. London, Ser. A*, 302, pp. 529-554.
- Brevik, I. and Aas, B. (1980): Flume experiment on waves and currents I. rippled bed, *Coastal Engineering*, 3, 1980, pp. 149-177.
- Brevik, I. (1980): Flume experiment on waves and currents II. smooth bed, *Coastal Engineering*, 4, 1980, pp. 89-110.
- Gade, H.G. (1958): Effects of a nonrigid, impermeable bottom on plane surface waves in shallow water, *Jour. Marine Research*, Vol. 16, No. 2, pp. 61-82.
- Goda, Y. and Suzuki, Y. (1976): Estimation of incident and reflected waves in random wave experiments, *Proc. 15th Conf. on Coastal Eng., ASCE*, 1976, pp. 828-845.
- Hunt, J.N. (1952): Viscous damping of waves over an inclined bed in a channel of finite width, *La Houille Blanche*, Dec., pp. 836-842.
- Ippen, A.T. (1966): *Estuary and coastline hydrodynamics*, Mc Graw-Hill Book Co., Inc., New York, USA.
- Iwasaki, T. and Sato, M. (1972): Dissipation of wave energy due to opposing current, *Proc. 13th Conf. on Coastal Eng., ASCE*, 1972, Vol. 1, pp. 605-622.
- Jonsson, I.G. and Thomas, G.P. (1978): Wave action and set-down for waves on a shear current, *Jour. Fluid Mech.*, Vol. 87, pp. 401-416.

Keulegan, G.H. (1950): Wave motion, chap. 11 of Engineering Hydraulics, John Wiley and Sons, Newyork, 1950.

Longuet-Higgins, M.S. and Stewart, R.W. (1961): The change in amplitude of short gravity waves on steady non-uniform currents, Jour. Fluid Mech., Vol. 10, pp. 529-549.

Longuet-Higgins, M.S. and Stewart, R.W. (1964): Radiation stress in waves, a physical discussion with applications, Deep-Sea Res., Vol. 11, pp. 529-562.

Nakano, S., Ito, N. and Fujihira, Y. (1989): Interaction between surface waves and soft mud in an uniform current, Proc. Coastal Eng., JSCE, Vol. 30, pp. 339-343 (in Japanese).

Otsubo, K. And Muraoka, K. (1986 a): Resuspension of cohesive Sediment by currents, Proc. 3rd International Symp. on River Sedimentation, Vol. III, 1986, pp. 1680 - 1689.

Sakakiyama, T. and Bijker, E.W. (1989): Mass transport velocity in mud layer due to progressive wave, Jour. Waterway, Port, Coastal and Ocean Eng., ASCE, Vol. 115, No. 5, pp. 614-633.

Shibayama, T. and An, N.N. (1993): A visco-elastic-plastic model for wave-mud interaction. Jour. of Coastal Engineering in Japan, Vol. 36, No. 1, pp. 67-89.

Sterling, G.H. and Strohbeck, E.E. (1973): The failure of the South Pass 70 "B" platform in hurricanes Camille, Proc. 5th Conf. on Offshore Technology, Houston, Texas, 1973, pp. 719-730.

Thomas, G.P. (1981): Wave-current interactions: an experimental and numerical study. Part 1. Linear waves, Jour. Fluid Mech., Vol. 110, pp. 457-474.

Tsuruya, H., Nakano, S. and Takahama, J. (1987): Interaction between surface waves and a multi-layered mud bed, Rep. Port and Harbour Res. Inst., Ministry of Transport, Japan, Vol. 26, No. 5, pp. 141-173.

Tubman, M.W. and Suhayda, J.N. (1976): Wave action and bottom movements in fine sediments. Proc. 15th Conf. on Coastal Eng., ASCE, 1976, pp. 1168-1183.

Whitham, G.B. (1974): Linear and nonlinear waves, A Wiley-Interscience Publication, John Wiley & Sons, New York, 636pp.